DESIGN OF A RESONANT STRIPLINE BPM
FOR THE IR-FEL PROJECT AT NSRL*

X. Y. Liu[1,2,†], M. Dehler[2], M. Bopp[2], A. Scherer[2], B. G. Sun[1]

[1]NSRL, University of Science and Technology of China, Hefei, P. R. China
[2]Paul Scherrer Institut, CH-5232 Villigen PSI, Switzerland

Abstract

This paper presents the design of a 476MHz resonant stripline beam position monitor (BPM) for an IR-FEL machine at NSRL. This type of BPM was developed based on stripline BPM by moving the coupling feedthrough closer to the short end downstream. This modification introduces a resonance that gives this BPM a better capability to detect lower beam currents compared to broadband devices like button and classical stripline BPM. Meanwhile the change is small enough to use the same type of electronics. In the following sections, the basic principle, nonlinear effect, sensitivity, the filtered sum and difference signals, and the mechanical design of this BPM will be mainly discussed.

INTRODUCTION

A tunable IR-FEL [1] user facility is under construction at NSRL, which can generate FEL radiation covering far-infrared range from 40 μm to 200 μm and mid-infrared range from 2.5 μm to 50 μm. The beam parameters of this facility are listed in Table 1.

Table 1: Electron Beam Parameters of IR-FEL

Parameter	Value
Beam energy	15–60 MeV
Bunch charge	1 nC
Bunch length (rms)	2–5 ps
Bunch repetition rate	59.5, 119, 238, 476 MHz
Macro pulse length	5–10 μs
Macro pulse repetition rate	20 Hz

This facility is planned to be installed in a $16 \times 10 \, \text{m}^2$ hall. Such a compact machine makes button type BPM the only choice for the basic BPM system due to the advantage of small size. The basic BPM system consists of 10 button BPMs [2] as standard devices to achieve a position resolution better than 50 μm; in addition, we plan to install another type of BPM near the energy analysis section with capability of higher induced signal level and so a better resolution.

The optimal choice is a resonant stripline BPM similar to the design that was proposed to satisfy the measurement of proton beams with extremely small current [3]. To make use of the existing electronics modules in 476 MHz, this value was chosen as the central resonant frequency. The design

quality factor Q of BPM is around 30 as a compromise between high signal intensity and a suitable damping time.

BASIC PRINCIPLES

Similar to stripline BPM [4], the cross section of resonant stripline BPM is shown in Fig. 1. R is the inner radius of the stripline, should be the same as the beampipe radius of 17.5 mm. T is the thickness of stripline electrode, D is the radial distance between stripline and vacuum chamber, and θ is the coverage angle of stripline electrode.
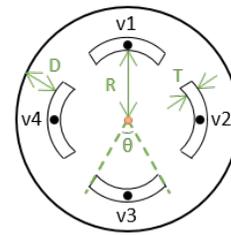

Figure 1: Cross section of stripline BPM.

The cross section contains one grounded chamber and four stripline electrodes inside, such that four different TEM modes exist:

- Sum mode (v1,v2,v3,v4) = (+1,+1,+1,+1);

- Dipole mode (v1,v2,v3,v4) = (+1,0,-1,0) or (0,+1,0,-1);

- Quadrupole mode (v1,v2,v3,v4) = (+1,-1,+1,-1).

Every stripline electrode and the grounded chamber form a transmission line. Its characteristic impedance Z, which can be calculated by using the Multipin Waveguide Port in CST [5], has the relation $Z \propto D/(\theta \cdot T)$ with varying parameters D, θ, and T.

The basic model of resonant stripline BPM is shown in Fig. 2a. The feedthrough divides the transmission line into two parts (length L1 and L2). When looking from the feedthrough port to both parts (marked as an arrow in Fig. 2), the part near the open end can be equivalent as a capacitor C_1, while the other part as an inductance L_{eff}. Then:

$$Z_{in}1 = -jZ \cot(\beta \cdot L1) = -j \frac{1}{\omega \cdot C_1}$$
$$Z_{in}2 = jZ \tan(\beta \cdot L2) = j\omega \cdot L_{eff}$$

(1)

Considering the parasitic capacitor C_p at the longitudinal gap (denoted as gap_z below) between the stripline and the vacuum pipe, the equivalent circuit can be simplified as the
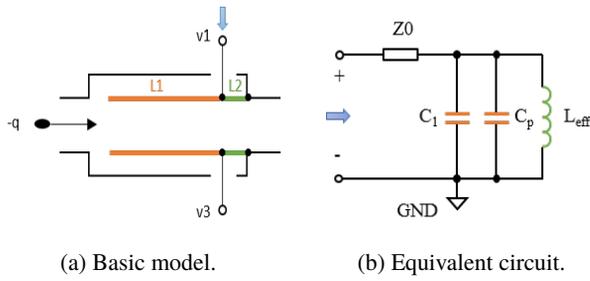
(a) Basic model. (b) Equivalent circuit.

Figure 2: Basic model of the resonant stripline BPM and its equivalent circuit when looking from the arrow as marked.

parallel LC circuit of Fig. 2b, where the total equivalent capacitance is $C_{eff} = C_1 + C_p$. In this circuit, Z0 is the characteristic impedance of feedthrough ($50\,\Omega$) and the inner losses along the transmission line are ignored. Accordingly, the resonant frequency f_0 and the external quality factor Q_e follows Eq. (2):

$$f_0 = \frac{1}{2\pi\sqrt{L_{eff} \cdot (C_1 + C_p)}}$$
$$Q_e = Z0\sqrt{\frac{(C_1 + C_p)}{L_{eff}}} \tag{2}$$

Based on Eq. (1) and the property of the C_p, each component of this equivalent circuit has a relation as:

$$C_p \propto \frac{\theta \cdot T}{gap_z}$$
$$C_1 \propto \frac{L1}{Z} \tag{3}$$
$$L_{eff} \propto Z \cdot L2$$

Moreover, due to the different coupling properties of these three types of mode, the characteristic impedance of them has the relation: $Z_{sum} > Z_{dipole} > Z_{quad}$. According to Eqs. (2) and (3), there should always exist two natural relations: $f_{sum} < f_{dipole} < f_{quad}$ and $Q_{e_{sum}} < Q_{e_{dipole}} < Q_{e_{quad}}$.

One design method is to choose the central frequency of post-processing system between f_{sum} and f_{dipole}, and a proper Q to ensure enough overlap but avoid the pathological case, in which the phase difference of these two modes at the selected frequency is 90 degrees [3].

Another method is to optimize all mode frequencies to a specific value by widening the coverage angle of half stripline upstream by an extra value θ_{add}. This option results in higher C_{eff} for all modes and relatively bigger effects on modes where electrodes have different potentials. This method was verified with the development for the SwissFEL Test Facility, Flash and EU-XFEL [6,7] and chosen here.

From the previous equations, we deduced the optimization rules summarized in Table 2. Based on these rules, the optimized mode frequencies f_0 and quality factors Q of our model via Eigenvalue Solver [5] are shown in Table 3.

Table 2: Optimization Rules

Option	Main effect
Fix L, decrease L2	Higher Q_e
Increase θ_{add}	Lower f_{sum}, f_{dipole} - f_{sum} and f_{quad} - f_{sum}
Increase gap_z	Higher f_0
Increase L	Lower f_0

Table 3: Simulated Mode Frequencies and Quality Factors of the Lossless Model with Ideal Feedthrough

Mode	f_0 [MHz]	$Q_e \approx Q_l$
Sum	476.07	31.03
Dipole	476.00	34.72
Quad	476.15	37.02

MECHANICAL DESIGN

The mechanical design of our BPM model including feedthroughs and flanges is shown as Fig. 3:
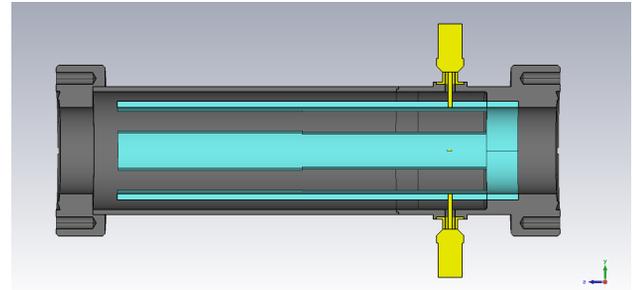

Figure 3: Mechanical Design of BPM model.

The material of vacuum chamber and stripline electrodes is stainless steel 316LN. The feedthrough was chosen as SMA type NL-108-564 [8] due to its compatibility with this BPM. The contact between the inner conductor of feedthrough and stripline electrode is ensured by welding. Termination of stripline at the downstream is effected by an extended circular piece, which will be also welded into the nearby flange. To ease the installation, at least one side of the BPM needs a rotating flange.

The final results of the mechanical model via Eigenvalue solver are shown in Table 4. Here, we considered the inner losses caused by materials and the change of vacuum pipe due to the introduction of real feedthrough geometry.

Table 4: Simulated Mode Frequencies and Quality Factors of the Mechanical Design

Mode	f_0 [MHz]	Q_e	Q_l
Sum	476.38	30.9	27
Dipole	476.20	34.5	29
Quad	476.42	36.7	31

MC6: Beam Instrumentation, Controls, Feedback and Operational Aspects

T03 Beam Diagnostics and Instrumentation

The Eigenvalue Solver was benchmarked using the CST Wakefield Solver [5], in which a single bunch with 1 nC charge and 2 ps rms length was located at a 2 mm offset. Based on this setting, the lowpass filtered sum and difference signals of output voltages from two opposite ports and their exponentially decaying envelopes were shown in Fig. 4, which also indicates a Q_{sum} of 27 and a Q_{dipole} of 29.
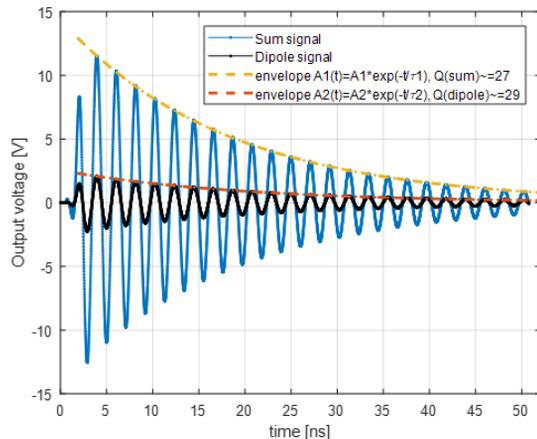

Figure 4: The lowpass filtered sum and difference signals of output voltages from two opposite ports.

Furthermore, the nonlinearity of position map was also studied. We kept the horizontal bunch position x at several specified values as 0 mm, 3 mm, 5 mm, 7 mm, 9 mm and 11 mm, then calculated the normalized position U_y by delta over sum method (as shown in Eq. (4)) for sweeping vertical displacements y within 5 mm. Figure 5 shows the linear fitting curves of U_y vs. y for different offsets x, which indicates that the sensitivity S_y (as shown in Eq. (4)) decreases with larger offsets x. Therefore in the case of large offsets, the higher order fitting equations need to be researched. The sensitivity S_y for $x = 0$ is around $0.0899\,\text{mm}^{-1}$.

$$U_y = \frac{v1 - v3}{v1 + v3}$$
$$S_y\,(\text{mm}^{-1}) = \frac{\partial U_y}{\partial y} \tag{4}$$

CONCLUSION AND OUTLOOK

This paper introduced the design of a 476MHz resonant stripline BPM. Its main advantages are the increased voltage level out of feedthrough due to the high Q and the compatibility with the existing electronics of button BPMs. Both of them make this BPM a good choice for a more precise beam position measurement in our machine.

The prototype will be built in the near future, after which the electrical properties should be tested first and following that tests with beam also.

This BPM might be also an option for non-interceptive emittance measurement considering its high Q_{quad} and the

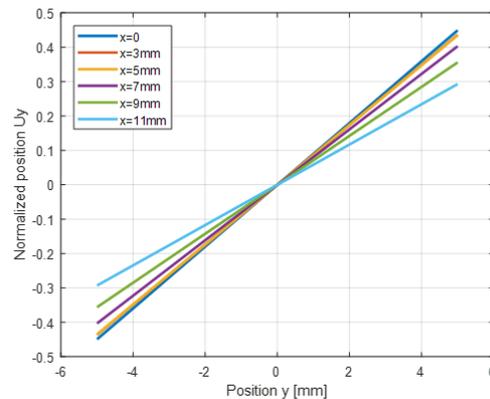Figure 5: Sensitivity curves for different offsets x.

existence of a triplet followed by a BPM in our facility, which was regarded as a stable implementation of Miller's emittance measurement method via 4-electrode-BPM [9, 10].

REFERENCES

[1] He-Ting Li *et al.*, *2017 Chinese Phys. C* 41 018102. doi: 10.1088/1674-1137/41/1/018102

[2] X. Y. Liu *et al.*, "Design and Simulation of Button Beam Position Monitor for IR-FEL", in *Proc. IPAC'16*, Busan, Korea, May 2016, pp. 187–189. doi:10.18429/JACoW-IPAC2016-MOPMB042

[3] M. Dehler, "Resonant Strip Line BPM for Ultra Low Current Measurements", in *Proc. DIPAC'05*, Lyon, France, Jun. 2005, paper POW021, pp. 286–288.

[4] T. Suwada *et al.*, "Stripline-type beam-position-monitor system for single-bunch electron/positron beams Nonintercepting emittance monitor". doi:10.1016/S0168-9002(99)00960-2

[5] Computer Simulation Technology. https://www.cst.com/

[6] M. Dehler, G. J. Behrmann, M. Siemens, and S. Vilcins, "Stripline Devices for FLASH and European XFEL", in *Proc. BIW'08*, Lake Tahoe, CA, USA, May 2008, paper TUPTPF013, pp. 110–114.

[7] A. Citterio, M. Dehler, B. Keil, V. Schlott, L. Schulz, and D. M. Treyer, "Design of a Resonant Stripline Beam Position Pickup for the 250 MeV PSI XFEL Test Injector", in *Proc. DIPAC'09*, Basel, Switzerland, May 2009, paper MOPD12, pp. 71–73.

[8] Hitachi Haramachi Electronics Ltd. https://www.hitachi.com/

[9] R.H. Miller, J.E. Clendenin, M.B. James, and J.C. Sheppard, "Nonintercepting emittance monitor". *United States: N. p.*, 1983. doi:10.2172/5746569

[10] S. J. Russell, "Unstable Matrix Equations and Their Relationship to Measuring the Emittance of an Electron Beam Using Beam Position Monitors", *Nuclear Instrument and Methods in Physics Research A 430*, 1999, pp.498-506.